JOURNAL OF COMPUTATIONAL PHYSICS 3, 379–398 (1969)

Numerical Computation of Steady, Supersonic, Two-Dimensional Gas Flow in Natural Coordinates*

FREDERICK P. BOYNTON AND ALEX THOMSON[1]

Convair Division of General Dynamics, San Diego, California 92112

Received April 19, 1968

ABSTRACT

A finite-difference technique useful for certain computations of hypersonic gas flows, with or without diffusion normal to the mean flow streamlines, is described. The scheme operates in the natural or intrinsic coordinate system and marches downstream from an input surface normal to the flow streamlines. The mesh is constructed by extending the streamlines according to the pressure distribution on the last available surface. The technique is explicit, and the usual stability restrictions on the stepping distance apply. Shock waves must generally be treated as discontinuties, although one can march through weak shocks with small loss of accuracy. Applications have been made to nozzle flows, to exhaust plumes, and to flows around bodies.

INTRODUCTION

This paper describes a finite-difference technique for solving steady, supersonic gas flow problems in two space dimensions. The technique is essentially a Lagrangian method, although it differs from the Lagrangian difference schemes previously reported in that fluid elements are followed through space rather than through time.

In the usual Lagrangian technique, the problem is treated by dividing the flow into elements at some initial time, and the subsequent motion and distortion of these elements is followed by marching along a time coordinate. This technique is easily applied [1, 2] to flow problems in one space dimension; however, when two-dimensional problems are attempted, problems often arise. If the fluid undergoes large distortion, as it might when velocities differ appreciably in the region of interest, the contortion of the fluid elements causes the differencing procedures which were adequate for the undistorted flow to become less accurate [3]. In the

* This work was sponsored by the Advanced Research Projects Agency, Project DEFENDER, through the Office of Naval Research, Contract Nonr 3902(00).

[1] Current address: Institute for Research and Technology, College of Engineering, Wayne State University, Detroit, Michigan.

present method, only the steady-state flow field is considered, and the marching is done along a space coordinate. Initial-value problems in this sense are properly posed if the gas is supersonic and if viscous stresses in the marching direction are negligible. We express the equations of motion in the natural or instrinsic coordinate system defined by the flow streamlines and the lines or surfaces normal to them. (These normal surfaces are potential surfaces in irrotational flow.) The calculation marches downstream, extending the streamlines and constructing new normal surfaces as it goes. Viscous transport normal to the streamlines is included. The technique is a fairly straightforward extension of the one-dimensional time-dependent techniques, but it does not appear to have received much attention in the past. Presumably, this lack of attention can be attributed to the widespread applicability of the method of characteristics, which in principle treats the same class of problems.

Our method was developed in order to compute the flow fields of rocket exhaust plumes at high altitudes (Fig. 1). The method of characteristics exhibits computational difficulties under these conditions, because the flow streamlines diverge and the Mach number is high. Characteristics of opposite family will eventually diverge unless the mesh size is refined, and the calculation cannot be carried to great distances from the nozzle in an efficient manner. In the shock layer which develops between the exhaust plume and the atmosphere, viscous mixing of the two streams take place. Since the shock layer is long and thin, viscous transport terms along the flow streamlines are small with respect to convective terms and can be neglected. Normal viscous transport should be included, as must the pressure differences required to turn the exhaust gases back along the flow centerline. In order to treat these flows, which involve large gradients normal to the streamlines, with a

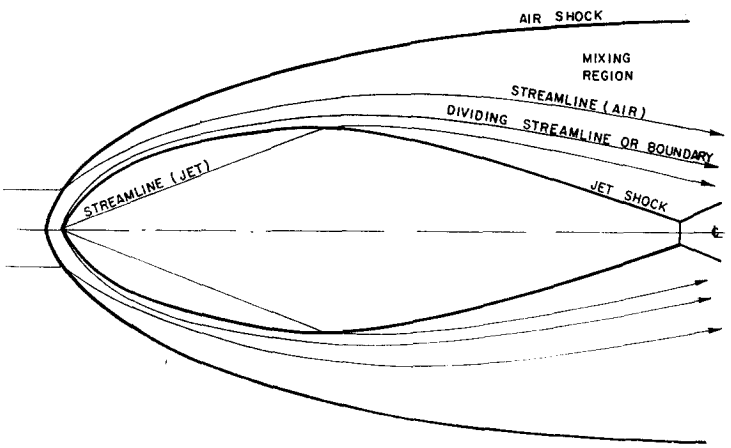

FIG. 1. High altitude exhaust plume flow field (schematic).

reasonable expenditure of computer time, it is desirable to employ techniques which converge rapidly to an acceptable solution as the number of mesh points is increased. The approach taken here is to embody as many of the conservation laws as possible in finding a solution, with the idea that if these fundamental relations are always satisfied the solution at least can never be unreasonable, and should generally be a satisfactory (if in some instances a coarse) representation of the real flow.

Because of the nature of the exhaust flow, where the structure inside the jet shock is identical to that which develops without any atmospheric interactions, it proves more convenient to compute the internal flow and the shock layer as two separate flows. The shocks are treated as discontinuities along the boundaries of the shock layer, and the jump conditions, together with the properties of the undisturbed exhaust and atmosphere, give the conditions just inside the boundaries. In this fashion the plume of a particular engine can be computed at several altitudes without repeating the internal undisturbed flow calculation and without introducing the complicated logic needed to treat the shock as an internal discontinuity. For this reason, as well as because some cursory attempts did not appear promising, there has been no extensive effort explicitly to introduce an "artifical viscosity" into the difference scheme.

We have applied the method to high-altitude exhaust plume calculations, to low-altitude plumes, to nozzle flows, and to flows around supersonic bodies. Exemplificative calculations for several of these flows are shown in a later section.

The natural coordinate system has several advantages:

1. in the limiting case of very large Mach number, the procedure reduces to the condition that the streamline curvature vanishes, and the solution is obtained trivially;

2. conservation equations may be used in integrated form (in inviscid flow), so that they are rigorously satisfied for any mesh spacing;

3. chemical reactions or internal relaxations may be easily incorporated, since the calculation follows fluid elements;

4. slip lines and large variations in fluid properties normal to the flow direction are treated without difficulty;

5. a wide variety of boundary conditions are easily accommodated;

6. species diffusion, shear, and heat transfer normal to the streamlines (the "thin viscous layer" approximation) are easily included;

7. since the calculation always marches in the flow direction, the difficulties encountered by Eulerian techniques when the flow direction and the marching direction differ appreciably are avoided.

The system also has some disadvantages:

1. methods based on it are generally of modest formal accuracy;

2. wave phenomena and their interactions are not as precisely defined as in the method of characteristics;

3. effects involving small portions of the total mass flow are not resolved unless the mesh size is made small in these regions;

4. because the mesh points must be located at each step, the procedure is less efficient than an Eulerian scheme with equivalent resolution. These advantages and disadvantages are common to Lagrangian techniques.

Development of the Difference Scheme

Consider the two-dimensional or axially symmetric flow of a nonreacting, viscous, heat-conducting, multicomponent fluid in which variations in velocity, temperature, and species concentrations are much larger in the direction normal to the flow than along it. Practical examples of such flows are the high-altitude shock layers of hypersonic vehicles [4] or exhaust plumes [5]. We write the equations describing this flow in the natural coordinate system (s, y) consisting of the flow streamlines and the surfaces normal to them, as follows:

Continuity:
$$\frac{\partial}{\partial s}(\rho u A) = 0; \tag{1}$$

Species Conservation:
$$\rho u \frac{\partial c_i}{\partial s} = r^{-\delta} \frac{\partial}{\partial y}(r^{\delta} J_i); \tag{2}$$

Streamwise Momentum:
$$\rho u \frac{\partial u}{\partial s} + \frac{\partial P}{\partial s} = r^{-\delta} \frac{\partial}{\partial y}(r^{\delta} \tau); \tag{3}$$

Normal Momentum:
$$\rho u^2 \frac{\partial \varphi}{\partial s} + \frac{\partial P}{\partial y} = 0; \tag{4}$$

Energy:
$$\rho u \frac{\partial}{\partial s}(h + \tfrac{1}{2}u^2) = r^{-\delta} \frac{\partial}{\partial y}\left[r^{\delta}\left(u\tau + q + \sum_i h_i J_i\right)\right]. \tag{5}$$

Here s is the distance along a streamline, y the distance normal to it; ρ the density, u the velocity, A the area of an infinitesimal streamtube, c_i the mass fraction of the i th species, J_i the mass flux of that species, P the pressure, τ the normal shear stress, φ the flow angle with the reference plane or symmetry axis, h the specific enthalpy, q the normal heat flux, and h_i the partial specific enthalpy of the i th species. The flux terms should be understood to represent fluxes across the flow streamlines. The metric r is the distance normal to the reference plane or symmetry axis, and $\delta = 1$ for axially symmetric flow and $\delta = 0$ for two-dimensional flow.

The continuity equation can be integrated along streamlines to give

$$\rho u A = \dot{m}(y) = \text{constant}, \tag{6}$$

where $\dot{m}$ is the mass flow in a particular streamtube.

The species continuity and energy equations may be similarly integrated if the flow is inviscid, giving

$$h + \tfrac{1}{2}u^2 = H(y) = \text{constant}, \tag{7}$$

where H is the total enthalpy, and

$$c_i(y) = \text{const.} \tag{8}$$

Furthermore, by use of the thermodynamic relation $dh = TdS + dP/\rho$, the streamwise momentum equation may be integrated (so long as we do not cross shocks) to give

$$S(y) = \text{constant}, \tag{9}$$

where S is the entropy.

Together with the equation of state, Eqs. (6)–(9) allow one to determine all the state variables once the streamlines have been located and the streamtube areas defined. This information is obtained from Eq. (4), which gives the streamline curvature, and thus in inviscid flow the truncation errors are limited to those introduced in handling the normal momentum equation. When the flow is viscous, the streamwise momentum, species conservation, and energy equations can no longer be integrated and must be treated in differential form; additional truncation errors may thus arise through the flux terms.

In formulating the finite-difference procedure, an effort has been made to retain a physically meaningful interpretation even when the mesh sizes are sufficiently large that the relation between derivatives and differences is somewhat obscure. For this purpose a Lagrangian coordinate system offers several advantages over an Eulerian system for evaluating hypersonic flow fields, even though it is often more complex and less efficient in terms of computing time per mesh point. In inviscid flow, the integrated forms of Eqs. (6), (7), and sometimes (9) are used, so that these are rigorously satisfied no matter how large a step size is used. When the flow is viscous, the calculation is arranged so that an increase of energy, momentum or species content in one streamtube is exactly balanced by losses in adjacent tubes, and thus the integrated relations are always satisfied over the entire flow.

The finite-difference procedure is set up as follows: The flow is divided into a finite number of streamtubes. Initial data, consisting of the local streamtube properties and the coordinates of the dividing streamlines, are fed in along an orthogonal surface. The calculation marches downstream, predicting the flow properties on a new orthogonal surface using the properties of the last previously calculated surface plus the boundary condition at each edge of the surface. The curvature $\kappa_{k,\ell} = \partial\varphi/\partial s$ of the kth streamline at the point where it intersects the ℓth surface is evaluated from the normal pressure gradient determined from

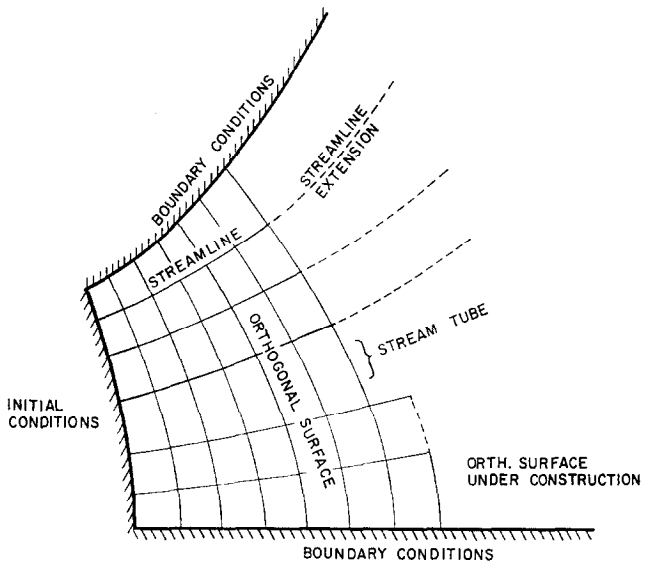

FIG. 2. Construction of flow field (interior zone); ---, trial; ——, final.

the pressures in the adjacent streamtubes (k and $k+1$, $k-1$ and k) on the ℓth surface (see Fig. 2). This curvature is used to extend the kth streamline to the $(\ell+1)$st surface. This procedure is repeated for each streamline. With the streamtube areas thus determined on the surface $\ell+1$, the state variables in each tube are evaluated from the conservation equations. When the flow is viscous, the fluxes of momentum, heat, and species are evaluated at the ℓth surface or halfway between surfaces ℓ and $\ell+1$ for use in determining the changes in c_i, H, and momentum between the ℓth and $(\ell+1)$st surface.

It is known that the straightforward application of this marching procedure is unconditionally unstable even in inviscid flow. However, it may be rendered stable by the following procedure: Having determined the state properties on the $(\ell+1)$st surface, the curvature $\kappa_{k,\ell+1}$ of the kth streamtube is evaluated from the pressure gradients on this surface. The surface $(\ell+1)$ is then recalculated using the weighted mean of the curvatures of the kth streamtube at the surfaces ℓ and $(\ell+1)$,

$$\bar{\kappa}_k = (1-\alpha)\,\kappa_{k,\ell} + \alpha\kappa_{k,\ell+1}\,. \tag{10}$$

Perturbation theory (acoustic approximation) shows that this procedure is stable when $\alpha > \frac{1}{2}$, unstable when $\alpha < \frac{1}{2}$, and neutrally stable when $\alpha = \frac{1}{2}$. In addition to this restriction in inviscid flow, the step length between surfaces must be chosen to be less than the separation between the streamlines k and $k \pm 1$ multiplied by a number of the order of $(M^2-1)^{1/2}$ where $M = u/a$ is the streamtube Mach

number. In viscous flow, the step length is also limited to a distance of the order of the separation times $Re_k = \rho u(\delta y)/\mu$ the streamtube Reynolds number. These two stepping limitations are not independent of each other, as we shall subsequently show.

In evaluating the streamline curvature, one wishes to use an expression that allows a reasonably accurate evaluation of the flow even when the values of the various state variables differ considerably from one tube to another, as in a flow behind a strongly curved shock or across a slip line. Since the computation time in flows with small viscous stresses is essentially inversely proportional to the square of the tube width, it is important to make the mesh size as large as allowed by the resolution desired in the results. In many hypersonic flows with slip lines and entropy layers, the entropy and density may each vary by an order of magnitude or more across a few tubes, while often flow velocity and curvature are relatively slowly varying. Equation (4) may be transformed to the form

$$\frac{\partial \varphi}{\partial s} + (2\pi r)^{\delta} \frac{\partial P}{\partial \dot{m}} = 0, \tag{11}$$

so that a useful representation of the curvature is

$$\kappa_k = -\frac{2(2\pi)^{\delta}(P_{k+1} - P_k)}{\dot{m}_k u_{k/r_k}{}^{\delta} + \dot{m}_{k+1} u_{k+1/r_{k+1}^{\delta}}}. \tag{12}$$

(We adopt the convention that the fluid properties indexed by k are those of the streamtube bounded by the kth streamline.) If the velocity and curvature are constant across the flow, Eq. (12) would give the correct curvature even if the entire flow were represented as one streamtube.

The streamlines are conveniently represented during a given step as arcs of circles, and the orthogonal surfaces are constructed by requiring that a line joining the intersections of adjacent streamlines with a given surface from an average right angle with the streamlines. The distance stepped and the streamtube areas are calculated along circular arcs with the proper tangencies at the end points.

In viscous flows, the species continuity, streamwise momentum, and energy equations are expressed as follows:

$$\dot{m}_k(c_{i,k,\ell+1} - c_{i,k,\ell}) = (2\pi)^{\delta} \Delta_k[r^{\delta} J_i \delta s], \tag{13}$$

$$\dot{m}_k(u_{k,\ell+1} - H_{k,\ell}) + \bar{A}(P_{k,\ell+1} - P_{k,\ell}) = (2\pi)^{\delta} \Delta_k[r^{\delta} \tau \delta s], \tag{14}$$

and

$$\dot{m}_k(H_{k,\ell+1} - H_{k,\ell}) = (2\pi)^{\delta} \Delta_k \left[r^{\delta}\left(u\tau + q + \sum h_i J_i\right) \delta s\right]. \tag{15}$$

Here the operator Δ_k takes the difference in the bracketed quantities across the kth streamtube. These expressions can be arranged so that all energy, momentum, or species mass leaving a given tube reappears in an adjacent tube, and initially isoenergetic flows with unit Lewis and Prandtl number remain isoenergetic. In this manner we ensure that the total mass and energy of the flow remain constant. In the momentum equation, $\bar{A}_k$ is the average streamtube area between surfaces ℓ and $\ell + 1$. We have found that representing $\bar{A}$ by the arithmetic average produces little change in streamtube entropy after several hundred steps in inviscid calculations, provided that the step size is controlled so that the change in area in a single step is less than about 10%. This accuracy restriction on the step size is generally less severe than the stability restrictions except in highly divergent flows.

It is desirable in evaluating the flux terms to employ expressions which keep the truncation errors as small as possible. The linear laws for the shear stress, heat flux, and (ordinary binary) species diffusion are

$$\tau = -\mu(\partial u/\partial y), \tag{16}$$

$$q = -k(\partial T/\partial y), \tag{17}$$

and

$$J_i = \rho D_{12}(\partial c_i/\partial y). \tag{18}$$

Our object is to produce from the difference equations the same values of τ, q, and J_i across a given streamline as we would have obtained from the differential equations. Two sources of error must be considered in passing to the finite-difference form: First, when the state properties differ by large amounts between two adjacent tubes, choosing a reasonable average value of the transport coefficient becomes difficult. Second, when streamtube areas or properties vary widely, it is hard to evaluate the gradients. The effects of these errors in the flux terms can be though of as producing a solution using erroneous transport properties, whose difference from the correct values is a function of position.

These difficulties can be reduced, though not altogether eliminated, by introducing the same transformation used in developing Eq. (12). (This transformation is similar to that of von Mises in boundary layer theory (6).) We may express Eq. (16), for example, as

$$\tau = (2\pi r)^{\delta} u(\rho\mu) \frac{\partial u}{\partial \dot{m}}. \tag{19}$$

The arguments previously introduced for hypersonic flows where u is not a rapidly varying function of position apply. Furthermore, the quantity $(\rho\mu)$ is not a strongly varying function of composition or temperature in gases; assuming that $(\rho\mu)$ is constant is an assumption often invoked in compressible laminar boundary layer theory. Therefore, since the pressure in steady unshocked flow usually varies

moderately slowly in the direction normal to the flow, a suitable finite-difference expression for the shear stress is

$$\tau_k = \overline{-2(2\pi r)^\delta u\rho\mu}\,\frac{u_{k+1} - u_k}{\dot{m}_{k+1} + \dot{m}_k}. \tag{20}$$

The barred term represents a mean transport coefficient whose value is in most situations rather insensitive to the averaging process employed. Usually $\dot{m}$ varies less from tube to tube than does tube width, so Eq. (20) is superior to the direct differencing of Eq. (16) in this respect also. Similar treatments can be applied to the fluxes of heat and species. Extension to situations in which multicomponent, pressure, and thermal diffusion are important is straightforward.

Stability

We noted previously that stability requires that the properties along a new orthogonal surface be calculated using the weighted mean of the curvature at the old and new surface. In this section we discuss this and other stability restrictions in more detail.

The inviscid equations may be represented by the wave equation as a linear analog,

$$v_{tt} = a^2 v_{xx}, \tag{21}$$

where a is the local wave velocity, here assumed constant, and subscripts now denote differentiation.

In finite-difference form, to second-order accuracy

$$v_t(t + \Delta t) = v_t(t) + a^2\,\Delta t v_{xx}(t + \Delta t/2) + O(\Delta t^2). \tag{22}$$

We introduce the weighting factor α as follows:

$$\begin{aligned} v_{xx}(t + \Delta t/2) &= \alpha v_{xx}(t + \Delta t) + [1 - \alpha]\, v_{xx}(t) \\ &= \alpha\left[v_{xx} + \frac{\Delta t}{2} v_{xxt}\right] + [1 - \alpha]\left[v_{xx} - \frac{\Delta t}{2} v_{xxt}\right] + O(\Delta t^2), \end{aligned} \tag{23}$$

where all derivatives are evaluated at $t + \Delta t/2$. Then, substituting in Eq. (22) and rearranging slightly,

$$\frac{1}{a^2} v_{tt} = \frac{v_t(t + \Delta t) - v_t(t)}{a^2 \Delta t} + O(\Delta t)^2 \tag{24}$$

$$= v_{xx}\left(t + \frac{\Delta t}{2}\right) + \Delta t\left[\alpha - \frac{1}{2}\right] v_{xxt}\left(t + \frac{\Delta t}{2}\right) + O(\Delta t^2). \tag{25}$$

Thus if $\alpha = \frac{1}{2}$, the term involving v_{xxt} drops out and the scheme is of second order accuracy.

We now postulate a perturbation to the solution of the form

$$v' = \exp\{-i\omega t - i\omega x/a\};$$

then, to terms of second-order accuracy,

$$\frac{1}{a^2} v'_{tt} = v'_{xx} - \left[\alpha - \frac{1}{2}\right] \Delta t \, i \frac{\omega^3}{a^2} v'. \tag{26}$$

Thus if $\alpha > \frac{1}{2}$, perturbations will be damped, while if $\alpha < \frac{1}{2}$, they will be amplified as the calculation progresses. In this sense, $[\alpha - \frac{1}{2}]$ may be thought of as an artificial viscosity, although no dissipation can occur in the inviscid scheme because of the required constancy of entropy. Calculations with various test flows confirm that when $\alpha > \frac{1}{2}$, perturbations (sound waves) are damped. In practical calculations, it is usually convenient and sometimes necessary to choose α slightly greater than $\frac{1}{2}$ in order to avoid perturbations introduced by small errors at mesh points or in boundary conditions. (A value of $\alpha = 0.55$ is generally satisfactory.) In most situations, properties vary only slowly along streamlines—i.e., over many steps. In this case, setting $\alpha > 1$ results in little loss of accuracy even though the formal accuracy is reduced to first order.

The second stability condition (step-size limitation) is developed in the usual way. In inviscid flow, the step size δs is related to the streamtube width δy by the von Neumann condition [1],

$$\delta s \leqslant \tfrac{1}{2}(M^2 - 1)^{1/2} \, \delta y. \tag{27}$$

Sample calculations in inviscid flows show that the allowed step size may be either greater or less than that allowed by Eq. (27), depending on local conditions, but is always nearly equal to it. It appears that the stability restriction for divergent flow is less stringent than that for convergent flow; the physical arguments involving Mach wave propagation across the mesh invoked to explain Eq. (27) would support this finding. In numerical work, we have tended to use a step size somewhat less than that of Eq. (27), with acceptable results.

In boundary-layer flows, whose transport terms resemble those in the thin viscous layer approximation, a stability criterion of the form

$$\delta s \leqslant \frac{1}{2} \frac{\rho u}{\mu} (\delta y)^2 = \frac{1}{2} Re_{\delta y} \, \delta y \tag{28}$$

restricts the stepping distance of explicit numerical procedures [7]. A similar restriction enters when our method is applied to supersonic viscous flows; however, an

interaction occurs between information propagation by Mach waves and diffusion which limits the step size to a value less than that allowed by either criterion alone. The case where $Re_{\delta y} = (M^2 - 1)^{1/2}$ has been examined, and we find that here

$$\delta s \leqslant \tfrac{1}{4}(M^2 - 1)^{1/2}\,\delta y = \tfrac{1}{4} Re\,\delta y. \tag{29}$$

We should expect that as the viscosity is reduced, holding M constant, the stepping distance approaches that of Eq. (27), and that if the viscosity is greatly increased, in the absence of nonlinear effects, the stepping distance approaches that of Eq. (28). A general relation providing an interpolation formula containing these three cases is

$$\delta s \leqslant \tfrac{1}{2}\,\delta y[Re^{-1} + (M^2 - 1)^{-1/2}]^{-1}. \tag{30}$$

Using a step size slightly less than that of Eq. (30) allows a successful solution to viscous flow problems. It should be recognized that this procedure is not a conclusive demonstration of a general stability relation. Since we have not derived a general stability criterion the only stability demonstration upon to us is an empirical one. Thus far, we have encountered no simple viscous flow problem for which a stepping distance 80 % of that given by Eq. (30) is unstable. However, when thermal and pressure diffusion are present, additional non-linear terms reduce the viscous stability limit; we still use Eq. (30) to choose the step size, but reduce the fraction by which the calculated stepping distance is multiplied to obtain the distance actually stepped.

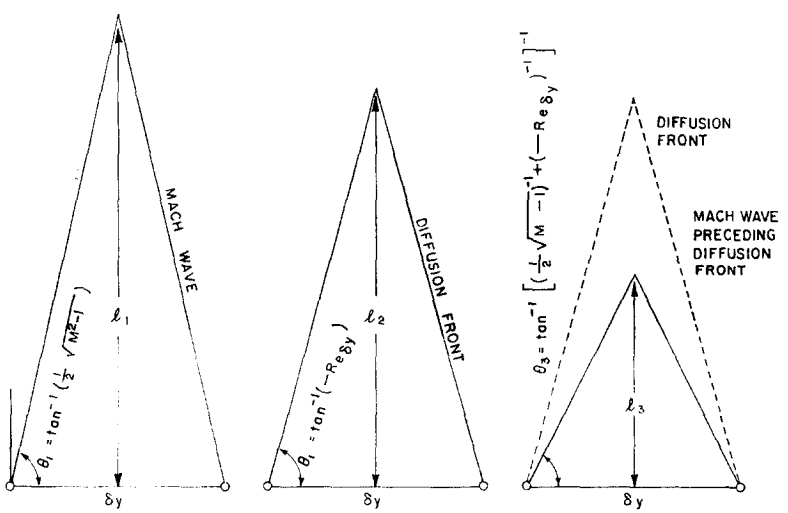

FIG. 3. Physical interpretation of stable stepping limits.

A straightforward physical argument may be introduced in support of Eq. (30). In Fig. 3(a) we consider an inviscid flow and show the Mach lines radiated from the intersections of the streamlines bounding the tube under consideration with the last calculated surface. The distance ℓ_1 to their intersection, as pointed out by von Neumann, is the upper limit to the stepping distance and is given by the equality in Eq. (27). In Fig. 3(b) we consider a purely diffusive flow and show the diffusion "fronts" propagating from the bounding points. (These fronts propagate linearly, instead of parabolically as in solutions to the differential equations, because of the form of the difference equation applied to a single step.) The distance ℓ_2 to their intersection is given by Eq. (29). Finally, in Fig. 3(c), both effects are shown together. Here we consider that a Mach wave propagates from the diffusion front, causing it to be felt to a greater distance than would be found in Fig. 3(b). The angle θ of the resulting distrubance is given by

$$\tan \theta = \{[\tfrac{1}{2}(M^2 - 1)^{1/2}]^{-1} + Re^{-1}\}^{-1} \tag{31}$$

and the distance ℓ_3 to the intersection of the disturbances propagated from the bounding points is given by Eq. (30).

Boundary Conditions and Shocks

A number of different boundary conditions can be treated fairly easily with this method. Since a solid wall or a symmetry axis is a streamline, one only has to demand that the innermost or outermost streamline follow the prescribed path. The shape of the boundary may be described either by an analytical expression or by a series of tabulated points. In the latter case, it is desirable to represent the boundary segments as arcs, rather than as straight lines, to reduce the perturbations caused by discontinuities in boundary slope at the junction points. A free boundary is easily treated by specifying the pressure along the bounding streamline and extending it in the usual way. When the external pressure is very low or zero, as in the case of expansion into a vacuum, the bounding streamline never quite turns to the limiting angle, although the limiting angle is more closely approached as the initial mesh near the edge is made smaller.

We noted earlier that, for our original application, it was more convenient to compute shocked flows sequentially, treating the shocks as boundary discontinuities propagating into a known flow field. Most of our calculations of shocked flows are performed in this manner. Consider the exhaust plume flow field as an example: Here there are two shocks, one propagating into the atmosphere and the other into the undisturbed jet flow. The properties of the atmosphere are uniform on the scale of the plume, and the external velocity vector is parallel to the centerline.

The shock properties are obtained by requiring that the shock turn the flow through as angle such that the downstream flow parallels the nearest streamline currently being carried in the computation. The resulting pressure behind the shock acts upon the outside of the nearest streamtube, as in the free-boundary calculation. The shock is extended downstream using the average of the shock angles at the old and new surface for each step. A similar procedure is followed for the jet shock; in this case, however, it is necesary to interpolate the properties upstream of the shock from the previously computed undisturbed jet flow.

Since the shock continually ingests the upstream flow, it becomes necessary from time to time to add a new streamtube to the flow being computed in the shocked region. The mass and enthalpy fluxes through the shock are summed from

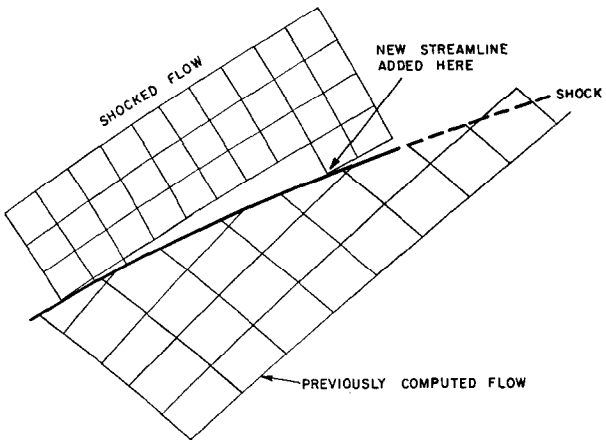

FIG. 4. Construction of flow field (shock region).

the last point at which a streamtube was added; when the mass flux approximates the average of those in the streamtubes then present in the flow, a new tube is added. The new tube's mass and enthalpy fluxes are those entering the shock, and the tube pressure is the pressure just behind the shock. In order to keep the number of streamtubes within reasonable bounds when computing a growing flow, it is necessary from time to time to combine tubes. We do this in a fashion which preserves bounding streamline angle, streamtube area at the given normal surface, mass and energy fluxes across the surface, and force exerted on the surface by the flow. The combination routine does not preserve total entropy flux when the tubes being combined have different state properties. The streamline pattern which results from the computation of a shocked region is shown in Fig. 4.

If the method is applied to a shocked region in which the shock is not treated by the above methods, the streamline pattern shown in Fig. 5 results. As in the

one-dimensional, unsteady calculation without artificial viscosity, the flow develops oscillations which (von Neumann pointed out) can be regarded as the calculation's attempt to simulate the conversion of kinetic energy to heat in the shock [2]. We did not note much improvement when Richtmeyer's artificial viscosity [1] and range of parameters were included in the calculation. Since $(\alpha - \frac{1}{2})$ is proportional to a sort of artificial viscosity, the oscillations will eventually damp

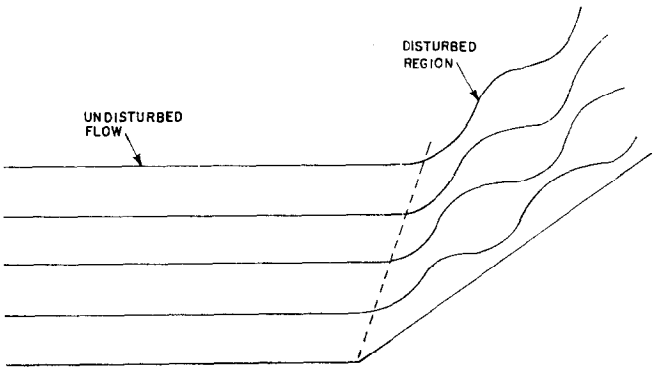

FIG. 5. Streamline pattern resulting from ignoring shock formation.

out if the calculation is carried far enough downstream. However, there is no indication that the far downstream flow has the proper state properties, although the flux quantities must be reasonable. In some cases, where the strongly shocked region is not of much interest, we have run calculations in which we simply march through it with low resolution in order to get at other parts of the flow; an example is shown in the next section.

SAMPLE CALCULATIONS

The areas of application of the method to inviscid flows are essentially equivalent to those of the method of characteristics. We have used it to compute flows in supersonic nozzles, of exhaust plumes and around supersonic bodies.

A typical axially symmetric nozzle flow is shown in Fig. 6. The heavy lines are streamlines, the light lines are isobars (shown as dotted lines where interpolation of the computer printout, which was requested only every 5 steps, is difficult). The coordinates are reduced by the throat radius. Only about $\frac{1}{4}$ of the computed streamlines are shown. The nozzle contour is a graphical approximation to an optimum-thrust contour. The calculation is initiated just downstream of the throat, assuming

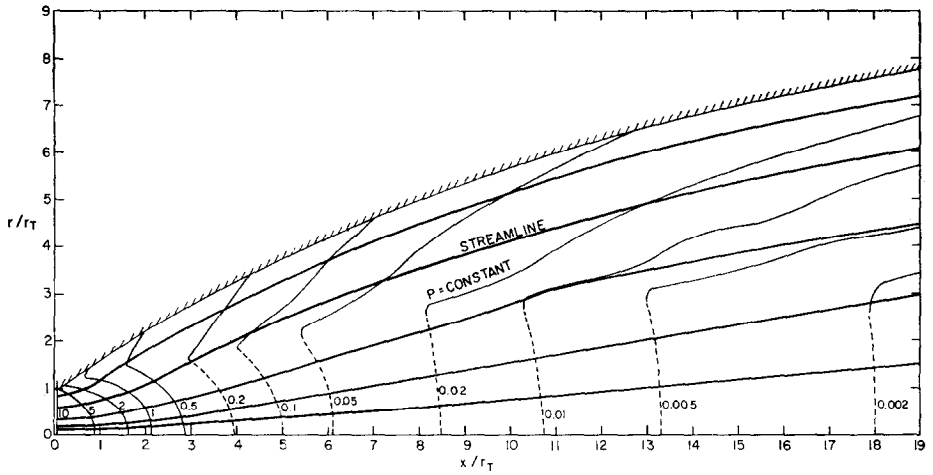

FIG. 6. Nozzle flow ($\gamma = 1.4$, $P_0 = 23.8$, $A/A^* = 60$).

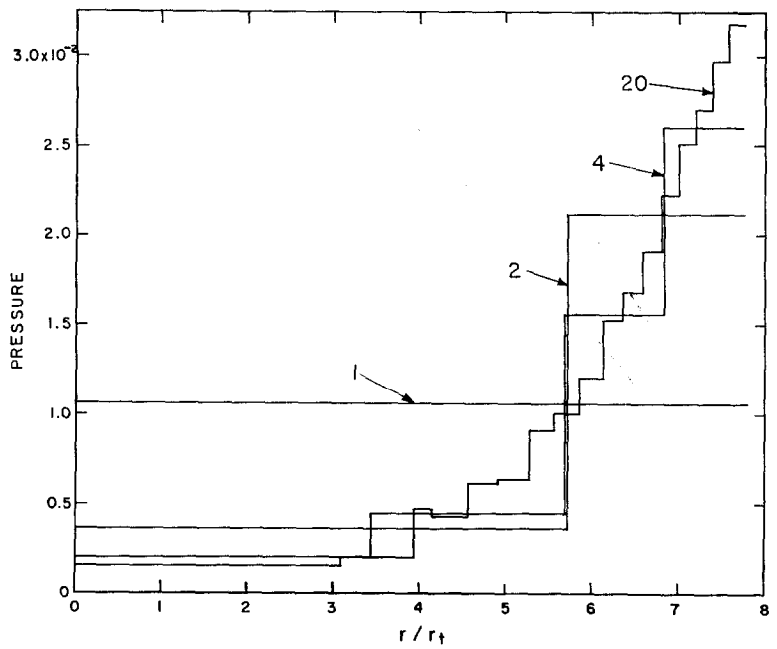

FIG. 7. Nozzle exit surface pressure profiles for different numbers of streamtubes in calculation.

slight irregularities in the nozzle contour as well as of the discontinuity in wall curvatures at the point where the contoured section joins the uniformly curved throat section [8]. This junction point induces a weak shock in the flow, which eventually strengthens as it approaches the axis. The isentropic calculation appears adequate for the region shown. This nozzle flow allows a good test of the contention that the flow results should be reasonable even if only a small number of tubes are employed. Figure 7 shows the pressure profile across the normal surface at the nozzle exit for 1, 2, 4, and 20 streamtubes in the calculation. With four tubes, the flow is reasonably well described; a line faired through the midpoints of these four tubes lies quite close to the results of the 20-tube calculation.

The undisturbed (vacuum) exhaust plume of this engine near the nozzle exit is shown in Fig. 8. The region at the lower right shows the typical streamline pattern which results when a shocked region is calculated without allowing for the shock. No attempt has been made to show the computed isobars here; they oscillate wildly. This shock system is induced by the nozzle, and includes not only the junction shock, but also a "focusing" shock consisting of the coalescence of many small compression waves induced by the contoured section and the reflections of these shocks from the axis. This reflection is actually irregular, with the formation of a Mach disc and a region of subsonic flow [9]. We march through this region by making the innermost streamtube large enough so that the flow within it remains, on the

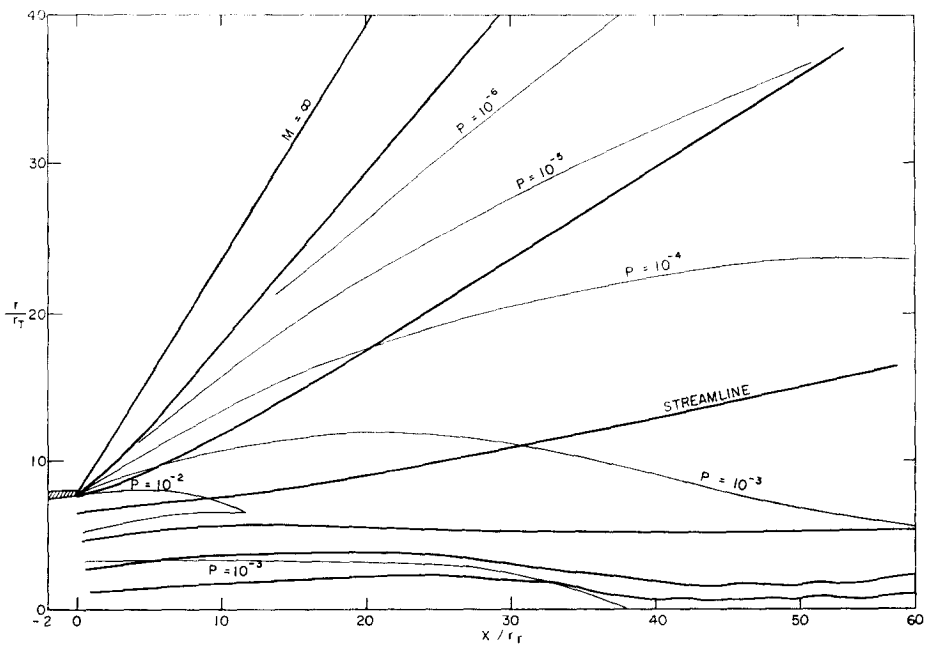

FIG. 8. Exhaust plume flow (near exit) into a vacuum; nozzle flow of Fig. 6.

average, supersonic. The percentage of the total mass flow which is strongly shocked is small, and the calculation satisfactorily describes the rest of the flow.

A comparison of two inviscid calculations of a low-altitude exhaust plume is still air is shown in Figs. 9 and 10. One calculation uses the method of characteristics [10] and the other uses our method. The jet shock and the slip line or boundary between jet and atmosphere is shown in Fig. 9. The pressure distribu-

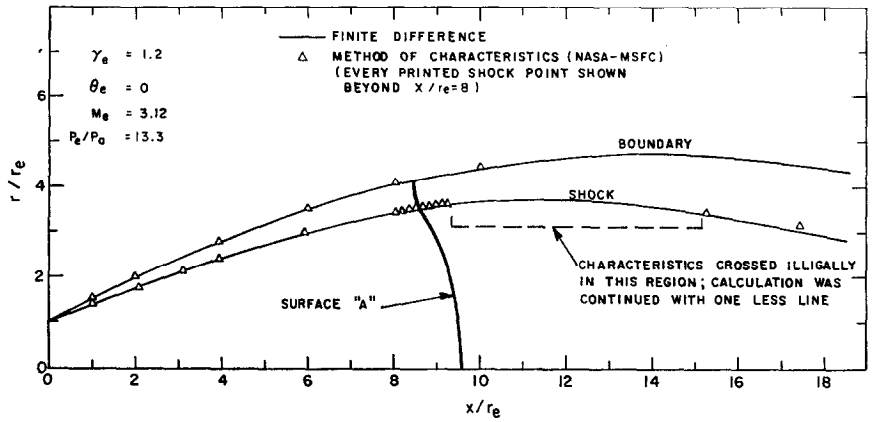

FIG. 9. Comparison of finite-difference and characteristics calculations; shock and boundary location.

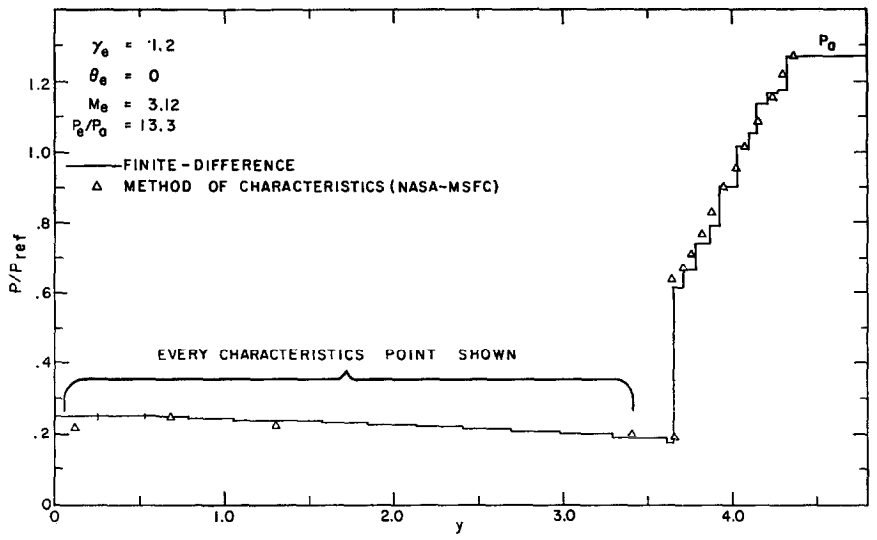

FIG. 10. Comparison of finite-difference and characteristics calculations; pressure profile along surface "A" of Fig. 9.

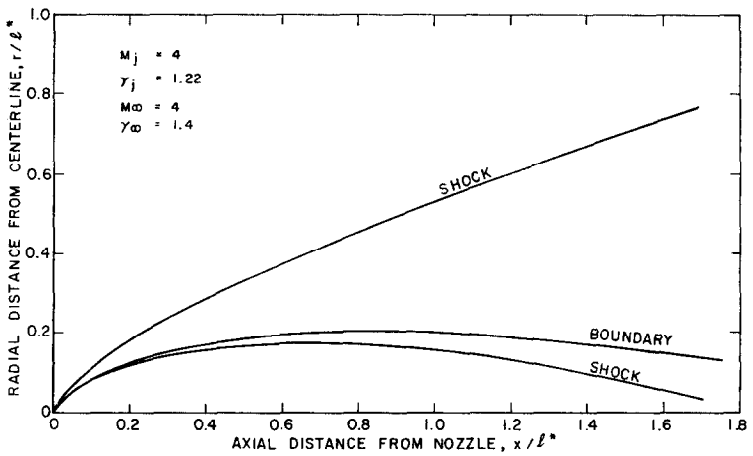

FIG. 11. High-altitude exhaust plume flow field; inviscid calculation.

tion across the surface "A" (of Fig. 9) normal to the flow streamline is shown in Fig. 10. The two calculations agree very well.

An inviscid high-altitude plume is shown in Fig. 11. The method of characteristics will not handle this problem without considerable effort. The air shock layer in the nose region is subsonic; an approximate method was used to compute the flow there to a distance slightly beyond the sonic line, which extends to a distance $x/\ell^* = 0.007$ from the exit plane. (Here ℓ^* is a characteristic scaling length for the high-altitude plume.) The entire jet flow, and the combined shock layer downstream, was computed with the present method. It has been shown that the computed exhaust-plume boundary location is very close to that given by approximate calculations involving a force balance along the boundary [11].

Calculations of the high-altitude plume with viscous transport have been presented elsewhere, both for binary diffusion and multicomponent diffusion [5, 12]. Applications to flow about a body have also been made [13].

CONCLUDING REMARKS

This method has been found to give satisfactory answers to a variety of problems involving supersonic and hypersonic flow fields. As is probably true of all numerical techniques, it is better suited to some problems than to others. In general terms,we believe that it is most reasonably applied to problems where moderate accuracy and physical reasonableness are desired in the answers, rather than to problems which require high precision in quantities such as shock location or wall pressure.

The question naturally arises, whether this method could be easily adapted to

three-dimensional steady flow problems. On the basis of a cursory investigation, we feel that it is in some ways less suitable than Eulerian or particle/fluid-in-cell techniques, since the three-dimensional surface normal to the flow streamline is difficult to construct and element contortion problems, like those occurring in two-dimensional, time-dependent Lagrangian calculations, can develop. Problems are often found in extending numerical techniques which rely entirely on a mesh which must be located in space as part of the calculation to three space dimensions. For example, efforts to develop a general three-dimensional method of characteristics have been under way for several years, but the number of problems successfully treated is, though growing, still relatively small. Many of the same difficulties, which arise entirely from the increased geometrical and topological complexity, also apply to our method. However, it is possible that some of these problems may seem more difficult than they really are, and the application of the method to some straightforward three-dimensional problem should probably be examined.

APPENDIX. NOMENCLATURE

A Streamtube area
a Acoustic or wave velocity
c Species mass fraction
D_{12} Binary diffusion coefficient
H Total enthalpy
h Static enthalpy
h_i Partial specific enthalpy
J Mass flux across streamlines
k Thermal conductivity
M Mach number
$\dot{m}$ Mass flow rate
P Pressure
q Heat flux across streamlines
r Distance normal to reference plane or symmetry axis
S Entropy
s Distance along streamline
T Temperature
u Velocity
y Distance along surface orthogonal to streamlines
α Weighting factor
Δ Difference operator
κ Streamline curvature
μ Viscosity

ρ Density
τ Shear stress (momentum flux across streamlines)
φ Flow angle

Subscripts and Exponents

i Species index
k Streamline or streamtube index
l Orthogonal surface index
δ Metric exponent ($= 0$ for $2-D$, $= 1$ for axially symmetric)

References

1. R. D. Richtmeyer, "Difference Method for Initial-Value Problems," Chap. 10. Wiley, New York (1959).
2. H. Geiringer, On numerical methods in wave interaction problems, *in* "Advances in Applied Mechanics," Vol. I, pp. 201–248. Academic Press, New York (1948).
3. W. D. Schultz, Two-dimensional Lagrangian hydrodynamic difference equations, *in* "Methods in Computational Physics," Vol. 3, pp. 1–45. Academic Press, New York (1964).
4. W. D. Hayes and R. F. Probstein, "Hypersonic Flow Theory," Chap. 7. Academic Press, New York (1959).
5. A. Thomson, High Altitude Rocket Plume Structure. [General Dynamics Convair Rept. GD/C-DBE65-023, September 1965.]
6. H. Schlichting, "Boundary Layer Theory," 4th ed., p. 136. McGraw-Hill, New York (1960).
7. S. L. Zeiberg and G. D. Bleich, Finite-difference calculation of hypersonic wakes. *AIAA J.* [illegible]
arc throat. *AIAA J.* **4**, 2219–2221 (1966).
9. J. M. Bowyer, Jr., L. D'Attore, and H. Yoshihara, Transonic Aspects of Hypervelocity Rocket Plumes; Supersonic Flow, *in* "Chemical Processes, and Radiative Transfer," pp. 201–210. Pergamon Press, London (1964).
10. R. C. Farmer, NASA George C. Marshall Space Flight Center, Huntsville, Alabama (private communication).
11. F. P. Boynton, Highly underexpanded jet structure: Exact and approximate calculation *AIAA J.* **5**, 1703–1704 (1967).
12. F. P. Boynton, The MULTITUBE Supersonic Flow Computer Code. [General Dynamics/Convair Report GD/C-DBE67-003, February 1967.]
13. F. P. Boynton, The Flow Field about a Long, Blunt-Nosed Body in Supersonic Flow. [General Dynamics/Convair Report GDC-ERR-AN-895, April 1966.]